

# Fatty liver in familial hypobetalipoproteinemia: triglyceride assembly into VLDL particles is affected by the extent of hepatic steatosis

Gustav Schonfeld,<sup>1,\*</sup> Bruce W. Patterson,<sup>\*</sup> Dmitriy A. Yablonskiy,<sup>†</sup> Tariq S. K. Tanoli,<sup>†</sup> Maurizio Averna,<sup>\*\*</sup> Nizar Elias,<sup>††</sup> Pin Yue,<sup>\*</sup> and Joseph Ackerman<sup>\*,†,§</sup>

Departments of Internal Medicine,<sup>\*</sup> Radiology,<sup>†</sup> and Chemistry,<sup>§</sup> Washington University, St. Louis, MO; Department of Medicine,<sup>\*\*</sup> University of Palermo, Italy; and Department of Internal Medicine-A,<sup>††</sup> B'nai-Zion Medical Center, Haifa, Israel

**Abstract** Familial hypobetalipoproteinemia (FHBL) subjects may develop fatty liver. Liver fat was assessed in 21 FHBL with six different apolipoprotein B (apoB) truncations (apoB-4 to apoB-89) and 14 controls by magnetic resonance spectroscopy (MRS). Liver fat percentages were  $16.7 \pm 11.5$  and  $3.3 \pm 2.9$  (mean  $\pm$  SD) ( $P = 0.001$ ). Liver fat percentage was positively correlated with body mass index, waist circumference, and areas under the insulin curves of 2 h glucose tolerance tests, suggesting that obesity may affect the severity of liver fat accumulation in both groups. Despite 5-fold differences in liver fat percentage, mean values for obesity and insulin indexes were similar. Thus, for similar degrees of obesity, FHBL subjects have more hepatic fat. VLDL-triglyceride (TG)-fatty acids arise from plasma and nonplasma sources (liver and splanchnic tissues). To assess the relative contributions of each, [<sup>2</sup>H<sub>2</sub>]palmitate was infused over 12 h in 13 FHBL subjects and 11 controls. Isotopic enrichment of plasma free palmitate and VLDL-TG-palmitate was determined by mass spectrometry. Nonplasma sources contributed  $51 \pm 15\%$  in FHBL and  $37 \pm 13\%$  in controls ( $P = 0.02$ ). Correlations of liver fat percentage and percent VLDL-TG-palmitate from liver were  $r = 0.89$  ( $P = 0.0001$ ) for FHBL subjects and  $r = 0.69$  ( $P = 0.01$ ) for controls. **Conclusion** Thus, apoB truncation-producing mutations result in fatty liver and in altered assembly of VLDL-TG.—Schonfeld, G., B. W. Patterson, D. A. Yablonskiy, T. S. K. Tanoli, M. Averna, N. Elias, P. Yue, and J. Ackerman. **Fatty liver in familial hypobetalipoproteinemia: triglyceride assembly into VLDL particles is affected by the extent of hepatic steatosis.** *J. Lipid Res.* 2003. 44: 470–478.

**Supplementary key words** nonalcoholic fatty liver • nonesterified fatty acids • very low density lipoprotein assembly • magnetic resonance spectroscopy

Familial hypobetalipoproteinemia (FHBL) is a genetically heterogeneous Mendelian dominant condition (1)

Manuscript received 26 August 2002 and in revised form 14 November 2002.

Published, JLR Papers in Press, December 1, 2002.

DOI 10.1194/jlr.M200342JLR200

that may be divided into at least four genetic subclasses: *a*) mutations of *APOB* (40 truncation-producing mutations ranging from apoB2 to apoB-89) (2–5); *b*) FHBL linked to chromosome 3p21 (6, 7); *c*) LDL receptor-deficient familial hypercholesterolemia in which a “cholesterol lowering gene” is linked to chromosome 13p (8, 9); and *d*) FHBL linked to none of the above loci (Schonfeld, unpublished observations). Most FHBL subjects are heterozygous and are usually asymptomatic, but an undetermined proportion have nonalcoholic fatty liver (NAFL) (5, 10–18). Since in several previous studies of liver fat the genetic classification of reported subjects was not specified, and in all studies a semi-quantitative measure of liver fat (ultrasound) was used, it is not clear how the specific genetic basis of FHBL affects either the frequency or severity of the fatty liver. We now report on liver fat in our group of subjects with the heterozygous form of FHBL due to *APOB* defects using a noninvasive quantitative method, magnetic resonance spectroscopy (MRS) (19–22). Since NAFL in humans is often associated with obesity and/or insulin resistance (23), we also measured indexes of obesity and insulin resistance in our FHBL subjects.

VLDL particles are assembled in liver from several apolipoproteins, the most important in humans being apoB-100, and the three major lipid classes: triglycerides (TG), cholesterol, and phospholipids. The TG component of VLDL particles is assembled from glycerol and fatty acids (FA). The FA incorporated into VLDL-TG may be derived from more than one source. Circulating nonesterified fatty acids (NEFA) may arise from lipolyzed adipose tissue

Abbreviations: ER, endoplasmic reticulum; FA, fatty acids; FHBL, familial hypobetalipoproteinemia; MRS, magnetic resonance spectroscopy; NAFL, nonalcoholic fatty liver; NEFA, nonesterified fatty acids; PR, production rate; TG, triglyceride; TTR, tracer/tracee ratio; Ra, rate of appearance.

<sup>1</sup> To whom correspondence should be addressed.

e-mail: gschonfe@im.wustl.edu

TG, and are transported in plasma complexed to albumin. FA also may arise from lipolyzed chylomicron-TG or VLDL-TG. These FAs are removed by liver and esterified into TG that may be assembled into VLDL-TG for export. FA may also be derived within liver by de novo synthesis (24–26). Mature VLDL particles are assembled in two steps (27): complexes form between lipids and apoB in the rough endoplasmic reticulum (ER) to form a primary VLDL particle, and these fuse with a separately formed “apoB-free” lipid particle fashioned in smooth ER (28). However, the relative contribution of plasma FA and nonplasma FA sources to the TG in these precursor particles and their subsequent assembly into VLDL-TG in vivo has not been studied in humans with FHBL. We hypothesized that there would be a positive correlation between the amount of fat detectable in liver by MRS and the relative contribution of nonplasma fatty acids to VLDL-TG. To assess the contribution of nonplasma sources, [ $^2\text{H}_2$ ]palmitate was infused as a representative fatty acid, and the extent of isotopic dilution between plasma [ $^2\text{H}_2$ ]palmitate and VLDL-TG palmitate was assessed by a compartmental model. Some of the results have been presented in abstract form (29, 30).

## METHODS

### Study subjects and protocols

The Washington University Human Studies Committee Studies approved our protocols, and informed consent procedures. No subjects were acutely ill or taking any medications known to affect lipid metabolism. None were diabetic, although a few had BMIs > 30. Controls were either unaffected married members of the FHBL families or unrelated volunteers. There was no history of hepatitis or alcohol abuse. Liver chemistry profiles were normal. The controls to the FHBL subjects were matched with respect to mean age, gender, and indexes of obesity. For both the MRS and infusion studies, subjects were instructed not to change their diets and to abstain from ethanol for at least 1 week before the studies. A dietician interviewed a subset of patients about dietary intake using a 7-day diary. MRS studies were performed after fasting overnight (10–12 h) in those cases where [ $^2\text{H}_2$ ]palmitate infusion studies were not performed. In those cases where infusions were done, the infusions were performed first, then subjects ate breakfast at 7–8 AM and underwent the MRS exam between 1–5 PM. To assess the effects of the time of day on MRS measurements five determinations of liver fat percentage by MRS were performed as indicated in Table 4 over a 24 h period in three FHBL and three control subjects. Meals were eaten as follows: breakfast at 9 AM, lunch at 1 PM, and dinner at 6 PM. To assess any longer-term changes, the liver fat percentage in five FHBL subjects was examined following an overnight fast over a period ranging from 18 days to several months.

### Magnetic resonance spectroscopy

All MRS data were collected on a 1.5T Siemens Magnetom Vision scanner (Siemens, Erlanger, Germany). A localized volume MR technique based on a double spin echo PRESS sequence (31) without water suppression was used. Accurate voxel localization was achieved by utilizing specially designed numerically optimized RF pulses (32). This not only improved voxel localization but also almost doubled the signal-to-noise ratio by improving

voxel profile. An outer volume suppression technique was used to eliminate possible contamination of the weak signal from liver fat by very strong signals from subcutaneous fat outside the volume of interest. Prior to volume localized data acquisition, an imaging protocol was performed that included acquisition of anatomical images and positioning of the spectroscopic voxel in the area of the liver. Ten signal averages were obtained over a 20 s period. Both the anatomical images and the spectroscopic data were obtained while subjects held their breath. Three  $2 \times 2 \times 2$  cm<sup>3</sup> voxels were examined in each subject. The coefficient of variation of replicate values of the triplicate determinations for 3 voxels was 1.5% (n = 31 MRS examinations). An example of anatomical image used for positioning of voxels is provided in Fig. 1, inset. Two data sets with spin echo times 23 ms and 53 ms were obtained from each voxel and used to evaluate the spin density for fat and water contributions. The MRS liver fat percentage was reported as the spin density of the aliphatic  $^1\text{H}$  signal divided by the sum of the spin densities of aliphatic plus water  $^1\text{H}$  signals.

Bayesian probability theory (33) was used for time-domain data analysis. The water and fat time-domain signals were each modeled as a sum of exponentially decaying sinusoids. The amplitude and frequency of each sinusoid were optimally estimated (along with the decay rate constant and phase). All frequencies, i.e., chemical shifts, were measured relative to the principal water  $^1\text{H}$  resonance, which was referenced as zero Hz. Typical frequency-domain linewidths of the water signal were in the range 30–35 Hz. Examples of  $^1\text{H}$ -MRS frequency domain spectra are provided in Fig. 1. The lipid signal resulted from multiple chemically shifted  $^1\text{H}$  resonances corresponding to methyl and methylene groups occupying different positions on lipid molecules with frequencies found in the range –140 Hz to –245 Hz (0.9–2.4 ppm) with major peak at about –220 Hz (~1.3 ppm) corresponding to methylene groups in (CH<sub>2</sub>)<sub>n</sub> chains (19, 21, 34). The sum total of the resonance amplitudes from both the methyl and methylene groups were used for calculation of hepatic triglyceride content. The residual of all modeling was always less than 1%.

To assess the comparability of chemical measurements of liver triglycerides and liver fat measured by MRS, the excised livers of six mice, wild-types and FHBL mimics engineered to harbor the apoB38.9 truncation (10), were examined by MRS using the same scanner and the same pulse sequence as for human studies. Lipids were extracted (35) and TG quantified by an enzymatic method (Wako, Richmond, VA). Fat content determined by chemical analysis in these mice ranged from 7 mg to 45 mg TG/gram wet liver. The regression of weight percentage liver TG (chemical) on MRS liver fat percentage was  $y = 0.807x$ ,  $R^2 = 0.986$ .

### VLDL-TG metabolic studies

Subjects were admitted to the Washington University General Clinical Research Center after a 10-h fast at about 6 PM. Intravenous catheters were inserted into the antecubital fossae of both arms, one for infusion, the other for venous blood sampling. [ $2,2\text{-}^2\text{H}_2$ ]palmitate (Cambridge Isotope Laboratories, Andover MA) infusions contained 0.341 g of potassium palmitate/100 ml of 25% sterile human serum albumin (molar ratio = 3.1), and were infused at 0.04  $\mu\text{mol/kg/min}$  for 12 h using an Ivac pump. [ $1,1,2,3,3\text{-}^2\text{H}_5$ ]glycerol (Cambridge Isotope Laboratories) was dissolved in sterile 0.9% saline and administered as a bolus (75  $\mu\text{mol/kg}$ ). Blood samples were obtained at 0, 5, 15, 30, and 60 min, then at 1.5, 2, 3, 4, 5, 6, 7, 8, 9, 10, and 12 h for the determination of plasma and VLDL-TG derived glycerol and palmitate isotopic enrichment. Plasma was separated by centrifugation within 30 min of sample collection. Two milliliters of fresh plasma was overlaid with  $d = 1.006$  g/ml EDTA-saline, spun in a 50.4 Ti

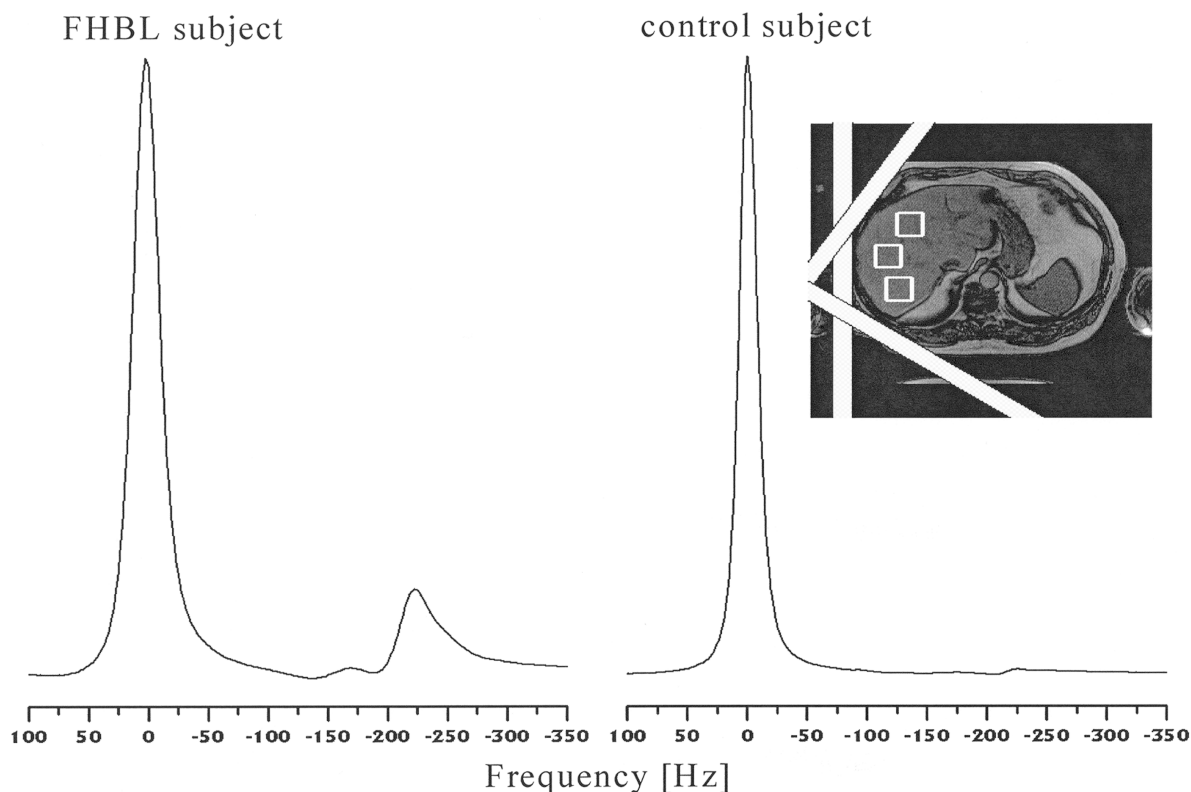


**Fig. 1.**  $^1\text{H}$ -magnetic resonance frequency domain spectra derived from hepatic voxels. Main peak in both graphs belongs to water signal and smaller peaks belong to triglycerides. Fat content in familial hypobetalipoproteinemia (FHBL) subjects is 18% and in control subject is 2%. The inset shows a magnetic resonance image of liver. The sites of three voxels are indicated by the boxes. The areas on the left side of the picture covered by the wide lines (saturation pulses) consist mostly of subcutaneous fat; these signals were suppressed so as not to contribute to the intrahepatic fat signals.

rotor at 40,000 rpm in a Optima LE80K ultracentrifuge (Beckman Instruments, Palo Alto, CA), and the VLDL fraction recovered by tube slicing. Remaining plasma was frozen at  $-70^\circ\text{C}$ .

### Isotopic analyses

Procedures to process plasma and VLDL-TG and measure the tracer/tracee ratio (TTR) of glycerol and palmitate have been previously reported (36, 37). The TTR of the heptafluorobutryl derivative of glycerol ( $m+5/m+0$  isotopomer ratio) and palmitate methyl ester ( $m+2/m+0$  isotopomer ratio) were measured by electron impact ionization gas chromatography/mass spectrometry (GC/MS) on a Hewlett-Packard (Palo Alto, CA) 5973 GC/MS system (37). Instrumental response was calibrated using standards of known isotopic enrichment.

### Kinetic modeling

The VLDL-TG metabolic kinetics using a bolus of  $[^2\text{H}_5]$ glycerol and an infusion of  $[^2\text{H}_2]$ palmitate was assessed using a compartmental model (36–38). Kinetic parameters were independently determined for glycerol and palmitate tracers. The model incorporates the time course of plasma glycerol and palmitate tracers, provides an excellent fit to the VLDL-TG glycerol/palmitate TTR time course, and provides an estimate of the fractional contribution from plasma versus nonplasma sources of VLDL-TG palmitate by accounting for the extent of isotopic dilution between the plasma palmitate and VLDL-TG. Although hepatic de novo lipogenesis may account for  $\sim 30$ – $50\%$  of the palmitate appearing in VLDL-TG during periods of high carbohydrate feeding (39, 40), de novo lipogenesis can be virtually undetectable and accounts for less than 5% of VLDL-TG palmitate during basal

fasting conditions such as those in our study (39–42). Thus, the isotopic dilution during fasted conditions is primarily due to the contribution from preformed palmitate from nonplasma sources, e.g., the splanchnic bed and liver. The VLDL-TG production rate (PR) was the product of the fractional catabolic rate (FCR) determined using the glycerol bolus tracer and VLDL-TG concentration. Compartmental modeling was performed using the SAAM II program (SAAM Institute, University of Washington, Seattle). The compartmental model accounts for any isotopic dilution of glycerol in liver and the recycling of tracer glycerol into a nonplasma glycerol pool that turns over and contributes to VLDL-TG production, causing the “tail” of the VLDL-TG glycerol enrichment to flatten out at the end. The model determines the true VLDL-TG FCR by resolving this recycling process, and thus the VLDL-TG production rate is determined by  $\text{FCR} \times \text{pool size}$ .

The rate of appearance (Ra) of palmitate into plasma was used as an index of the rate of whole-body lipolysis and delivery of fatty acids to the liver for VLDL-TG production. Palmitate Ra was evaluated using the steady-state Steele equation (43) as modified for use with stable isotopes (44):  $\text{Ra} = I/\text{TTR}$ , where I = rate of tracer palmitate infusion ( $\mu\text{mol}/\text{kg}/\text{min}$ ).

### Indexes of obesity and insulin resistance

Body mass (kg) and height (m) were measured and the BMI ( $\text{height}/\text{body mass}^2$ ) calculated. Waist and hip circumferences were measured, and waist to hip ratios were calculated. Two-hour oral glucose tests using 75 gm of glucose and measurements of plasma glucose and insulin were obtained using standard methods after the MRS study in the morning or on a different morning a few days later. AUC for glucose and insulin and a fasting



HOMA index for insulin resistance were calculated using fasting values of glucose and insulin (45).

### Statistical analysis

Statistical analyses used SAS/STAT (SAS Institute, Gary, NC). Pearson or Spearman correlation coefficients were used as appropriate. Log transformation of liver fat percentage was used since it was not normally distributed. The Chi-square test was used to compare sex differences among groups, and the Kruskal-Wallis to compare age differences. The ANOVA (Duncan's multiple range test) was used to compare means of subject groups ( $P \leq 0.01$ ). Multivariate stepwise regression was used with MRS liver fat percentage or log liver fat percentage as the dependent variable. Male gender was assigned a value of zero and females of one. Results shown are mean  $\pm$  SD.

## RESULTS

### Study subjects

Demographic characteristics are provided in **Table 1**. Twenty-one simple heterozygous subjects and one compound heterozygous female (with an apoB<sup>40/89</sup> genotype) participated. They represented various apoB truncations (**Table 2**). The original references describing the mutations are provided in Table 2. Table 2 also lists the subjects who participated in the MRS study, in the palmitate infusion study, or in both.

The eight families from which the 22 affected subjects volunteered for the protocols form part of a larger group of 14 St. Louis FHBL families. The seventy-one additional FHBL affected subjects who did not undergo MRS analysis resembled the 22 FHBL subjects who did, with respect to lipoprotein levels, age, gender, and indexes of body weight (Table 1). The 22 FHBL subjects and the 15 controls differed with respect to apoB and LDL-cholesterol (LDL-C) by definition but not with respect to age, gender and indexes of insulin resistance or obesity (Table 1).

TABLE 1. Subject characteristics

	FHBL Studied Group	MRS Control Group	FHBL Control Group
Age (years)	44 $\pm$ 16	40 $\pm$ 14	40.7 $\pm$ 19.6
Number (gender)	22 (11 M:11 F)	16 (8 M:8 F)	71 (47 M:24 F)
BMI (kg/m <sup>2</sup> )	26 $\pm$ 4	26.8 $\pm$ 4.7	25.9 $\pm$ 6.2
Waist (cm)	90 $\pm$ 13	87 $\pm$ 17	
Waist/hip ratio	0.87 $\pm$ 0.09	0.82 $\pm$ 0.09	
Total TG (mg/dl)	60.4 $\pm$ 58.1	55.5 $\pm$ 39.8	68.4 $\pm$ 47.1
VLDL TG (mg/dl)	48.3 $\pm$ 54.2	42.5 $\pm$ 33.5	40.3 $\pm$ 31.3
Total cholesterol (mg/dl)	109 $\pm$ 29	184 $\pm$ 31	108.2 $\pm$ 27.3
VLDL-cholesterol (mg/dl)	10 $\pm$ 12	15 $\pm$ 14	10.0 $\pm$ 13.6
LDL-cholesterol (mg/dl)	44 $\pm$ 18 <sup>a</sup>	117 $\pm$ 26 <sup>a</sup>	42.3 <sup>a</sup> $\pm$ 18.7
HDL-cholesterol (mg/dl)	55 $\pm$ 20	51 $\pm$ 14	52.1 $\pm$ 13.7
ApoB (mg/dl)	26 $\pm$ 15 <sup>a</sup>	80 $\pm$ 17 <sup>a</sup>	34.5 <sup>a</sup> $\pm$ 17.1
ApoA-I $\pm$ SD (mg/dl)	127.9 $\pm$ 30.9	117.7 $\pm$ 21.1	135.8 $\pm$ 25.2
AUC-glucose (mg/dl/min)	660 $\pm$ 317	452 $\pm$ 359	
AUC-insulin ( $\mu$ /ml/min)	605 $\pm$ 255	381 $\pm$ 340	
Fasting HOMA	1.39 $\pm$ 0.99	1.32 $\pm$ 1.06	

Mean  $\pm$  SD.

<sup>a</sup> Comparisons were made among means of the three groups with Duncan's multiple range test, overall  $P$  level = 0.01. For all other comparisons  $P > 0.2$ .

TABLE 2. Fraction of VLDL-TG-palmitate derived from hepatic stores

Study Subjects	ApoB Genotype	References to Original Description	VLDL-TG-Palmitate Derived from Nonplasma Palmitate (Model)	Liver Fat Percentage (MRS)
<b>Affected</b>				
T1	B-4/B-100	(56)	0.76	31.1
T2	B-4/B-100	(56)	0.62	18.9
T10	B-4/B-100	(56)	0.64	19.4
T11	B-4/B-100	(56)	0.51	18.0
T12	B-4/B-100	(56)	0.38	ND
T16	B-4/B-100	(56)	0.44	2.3
MR36	B-4/B-100	(56)	ND	3.6
MR32	B-9/B-100	(57)	ND	17.2
MR33	B-9/B-100	(57)	ND	13.2
MR35	B-9/B-100	(57)	ND	17.2
MR52	B-29/B-100	(58)	ND	36.5
MR26	B-31/B-100	(59)	ND	8.4
T17	B-52/B-100	(60)	0.58	17.3
T18	B-52/B-100	(60)	0.22	4.4
T21	B-52/B-100	(60)	0.38	1.6
T22	B-52/B-100	(60)	0.43	3.9
MR31	B-52/B-100	(60)	ND	6.7
T13	B54.8/B-100	(61)	0.40	1.7
MR29	B-75/B-100	(62)	ND	14.1
T3	B-40/B-89	(63)	0.71	31.7
T19	B-89/B-100	(63)	0.52	24.1
T20	B-89/B-100	(63)	0.53	15.1
Mean $\pm$ SD			0.51 $\pm$ 0.15	16.7 $\pm$ 11.5
<b>Controls</b>				
T4	B-100/B-100		0.34	ND
T5	B-100/B-100		0.38	3.7
T6	B-100/B-100		ND	3.4
T7	B-100/B-100		0.34	2.3
T8	B-100/B-100		0.26	1.2
T9	B-100/B-100		0.33	2.2
T14	B-100/B-100		0.45	9.3
T15	B-100/B-100		0.30	0.5
T23	B-100/B-100		0.22	1.1
T24	B-100/B-100		0.43	7.3
T25	B-100/B-100		0.40	1.0
T26	B-100/B-100		0.32	0.4
MR41	B-100/B-100		ND	1.1
MR46	B-100/B-100		ND	1.8
MR47	B-100/B-100		ND	5.4
MR48	B-100/B-100		ND	7.3
Mean $\pm$ SD			0.37 $\pm$ 0.13	3.3 $\pm$ 2.9
<i>P</i>			0.002	<0.001

ND, not done.

### Fatty liver

Mean MRS liver fat percentage of FHBL subjects were 5-fold higher than in controls (16.7  $\pm$  11.5 vs. 3.3  $\pm$  2.9, respectively,  $P < 0.001$ ) (Table 2). However, there were substantial overlaps between control and the lower FHBL values. Log liver fat percentage was significantly positively correlated with BMI, waist, and insulin AUC in FHBL subjects, and was higher in male than female FHBL subjects. A similar pattern of correlations was seen in controls (**Table 3**). On multivariate analysis of the combined groups, significant predictors of liver fat percentage were gender, BMI, and LDL-C ( $R^2 = 0.44$ ,  $P = 0.002$ ). For the FHBL group, gender and LDL-C were the most important predictors ( $R^2 = 0.65$ ,  $P = 0.004$ ). Thus, for a given BMI or waist circumference the liver fat content of FHBL subjects were higher than controls.

TABLE 3. Correlation coefficient between liver fat content and the indicated parameters

	Log (Liver Fat Percentage) versus FHBL	Log (Liver Fat Percentage) versus Controls
Gender <sup>a</sup>	-0.45 <sup>b,c</sup> (-0.43)	-0.62 <sup>c</sup> (-0.63 <sup>b</sup> )
BMI	0.49 <sup>b</sup> (0.51 <sup>c</sup> )	0.60 <sup>b</sup> (0.60 <sup>b</sup> )
Waist	0.48 <sup>b</sup> (0.59 <sup>c</sup> )	0.73 <sup>c</sup> (0.71 <sup>b</sup> )
AUC-insulin	0.49 <sup>b</sup> (0.46)	0.30 (0.35)
Fraction VLDL-TG palmitate derived from nonplasma sources	0.77 <sup>e</sup> (0.89 <sup>c</sup> )	0.50 (0.69 <sup>b</sup> )
VLDL-TG glycerol production rate	-0.01 (0.08)	0.16 (0.27)

Pearson coefficients are shown, Spearman correlation coefficients are listed in parentheses.

<sup>a</sup> Gender was coded as 0 for male, and 1 for female.

<sup>b</sup> Statistically significant at  $P < 0.05$ .

<sup>c</sup> Statistically significant at  $P < 0.02$ .

<sup>d</sup> Statistically significant at  $P < 0.01$ .

<sup>e</sup> Statistically significant at  $P < 0.0001$ .

Liver contents varied over 24 h by ~10% (Table 4). Liver contents in FHBL subjects measured over several months varied by ~30% but levels remained high with each determination (Table 5).

**[<sup>2</sup>H<sub>2</sub>]palmitate infusions: palmitate fluxes, VLDL-TG assembly**

Plasma palmitate TTR achieved plateau values within 2 h and remained relatively constant thereafter (Fig. 2,

TABLE 4. Diurnal variation in liver fat contents

Patient Number	Status	Date of Study	Time	Mean Fat Percentage	SD
T26	control	11/17/01	7 AM	2.8	0.5
			12 PM	0.9	0.9
			5 PM	0.7	0.5
			10 PM	0.6	0.6
			7 AM	0.8	0.6
T8	control	01/12/02	7 AM	1.9	0.3
			12 PM	1.1	0.3
			5 PM	0.9	0.2
			10 PM	0.9	0.4
			7 AM	0.9	0.3
T9	control	01/12/02	7 AM	8.3	9.0
			12 PM	2.9	0.9
			5 PM	5.1	1.4
			10 PM	5.3	7.0
			7 AM	1.8	0.6
MR35	apoB-9	03/23/02	7 AM	27.8	1.0
			12 PM	34.7	1.4
			5 PM	29.8	2.1
			10 PM	30.4	2.5
			7 AM	29.0	1.3
T2	apoB-4	04/27/02	7 AM	21.5	1.1
			12 PM	20.9	0.4
			5 PM	21.2	0.6
			10 PM	21.4	3.4
			7 AM	21.9	1.3
MR36	apoB-4	05/18/02	7 AM	1.6	0.6
			12 PM	2.4	0.5
			5 PM	1.8	0.8
			10 PM	1.1	0.8
			7 AM	2.1	0.1

Results are means and SD of liver fat percentage determinations in three nonoverlapping voxels.

TABLE 5. Liver fat contents of FHBL subjects measured several months apart

FHBL Subject	ApoB Truncation	Date of MRS Analysis	Liver Fat Percentage
T1	B-4	10/08/00	34.1
		06/09/01	47.7
T2	B-4	10/08/00	33.1
		06/09/01	30.9
		04/27/02	21.5
T10	B-4	10/22/00	22.5
		06/09/01	29.4
T11	B-4	10/22/00	18.5
		06/09/01	24.9

upper curves). Mean palmitate flux rates (Ra) were identical in control ( $2.19 \pm 0.53 \mu\text{mol/kg/min}$ ) and FHBL subjects ( $2.19 \pm 0.67 \mu\text{mol/kg/min}$ ;  $P = 0.81$ ).

VLDL-TG palmitate TTR approached a plateau around 10 h (Fig. 2, lower curves). Nonplasma sources contributed  $37 \pm 13\%$  of VLDL-TG palmitate in control subjects and  $51 \pm 15\%$  in FHBL subjects ( $P = 0.002$ ) (Table 2). There were significant positive correlations between the relative contribution of nonplasma sources and liver fat percentage for FHBL ( $r = 0.890$ ,  $P = 0.0001$ ) and for the control ( $r = 0.691$ ,  $P = 0.018$ ) (Table 3, Fig. 3). However, the linear regression lines differed for the two groups, even when one seeming outlier control subject was omitted from the calculation (Fig. 3). The slope of the line for the control group did not differ from zero, but the slope for FHBL did differ from zero. On multivariate analysis, the fraction of VLDL-TG-palmitate derived from nonplasma sources was the most important determinant of liver fat content for FHBL subjects. This was not true for controls.

The VLDL-TG FCR, determined with the bolus injected glycerol tracer, was not significantly different between FHBL subjects and controls (Table 6). However, the apparent VLDL-TG FCR determined with the infused palmitate tracer was significantly slower for FHBL subjects compared with controls (Table 6). These differences between

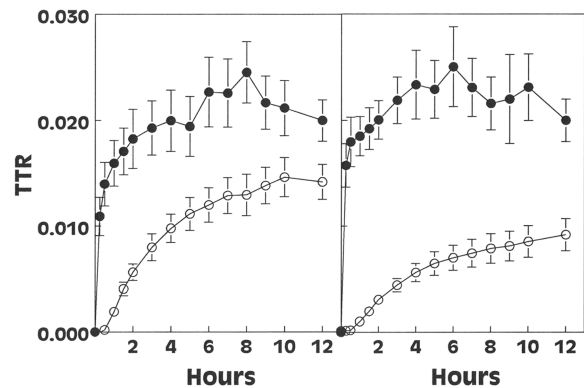
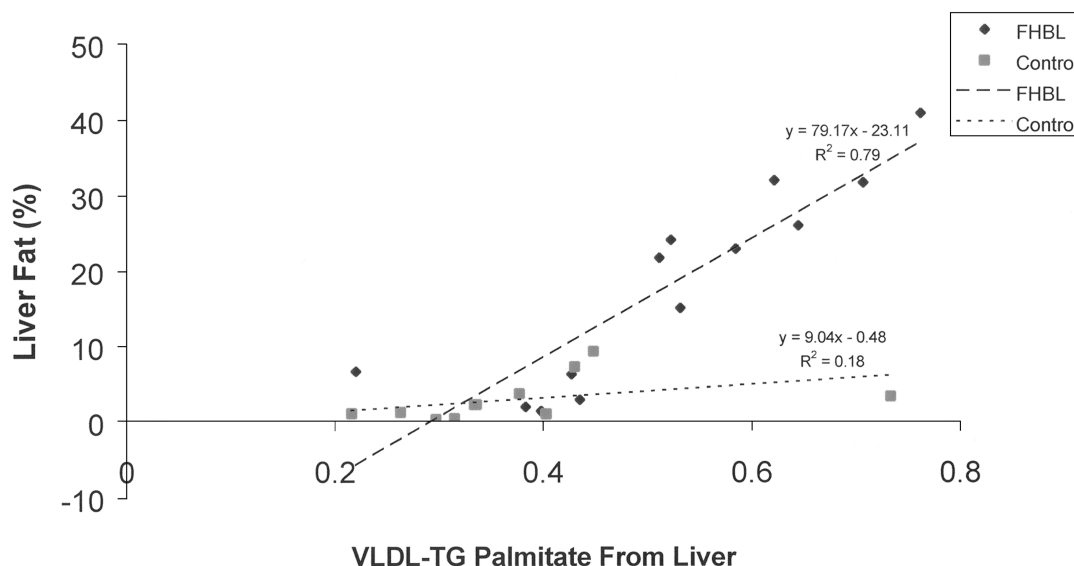


Fig. 2. Time course for enrichment of plasma and VLDL-TG [<sup>2</sup>H<sub>2</sub>]palmitate. The tracer/tracee ratio of plasma (solid symbols) and VLDL-TG (open symbols) is displayed for control subjects (left panel) and FHBL subjects (right panel). Results shown are group means  $\pm$  SEM.



**Fig. 3.** Regression of tracer-derived estimate of the contribution of liver fat to VLDL-TG-palmitate on liver fat percentage content as measured by MRS in FHBL and controls. If the control subject in the lower right hand corner of the figure is omitted, the regression becomes  $y = 31.32x - 7.82$ ,  $R^2 = 0.57$ .

bolus glycerol and infused palmitate have been previously noted (37). VLDL-TG PR computed from the glycerol data tended to be lower in FHBL. VLDL-TG PR were not computed for the infusion palmitate data because we believe them not to reflect the “true” production rates, for reasons set out in the discussion.

## DISCUSSION

Mean MRS liver fat percentage contents of FHBL subjects were 5-fold higher than controls (Table 2). If two standard deviations above the mean for the controls is used as a cut point, ~60% of *APOB*-defective FHBL subjects had fatty livers. These MRS data provide at least an initial estimate of the prevalence of fatty liver in FHBL of this genotype, since the 22 FHBL subjects surveyed for liver fat were drawn from some of the same families as the 71 FHBL subjects whose liver fat contents were not determined, and resembled them in a number of ways (Table 1). It is worth pointing out that the severity of fatty liver is less in subjects with another genetic form of FHBL that linked to chromosome p321 (6, 7) (Schonfeld, et al., unpublished observations). We have also documented that the apoB-100 and VLDL-TG production rates of the 3p21 subjects are less severely depressed than those of subjects bearing truncations of apoB (36, 38). These data suggest that the different FHBL genotypes may result in different phenotypes with respect to hepatic steatosis and VLDL kinetics.

Liver fat contents vary relatively little over 24 h in those with high levels of liver fat. Variations are larger in those subjects with low fat contents (Table 3). There are at least three potential sources of variation in these studies. First, based on analyses of signal to noise ratios, the minimum amount of fat that can be accurately quantified is ~0.5%.

Thus, small changes in the absolute fat contents of livers containing small amounts of fat may result in large percentage variations. Second, the variations may reflect real regional differences in fat contents of the liver. This is shown in Table 4, where mean values for the three adjacent, but noncontiguous voxels measured are provided (see SDs). Intrahepatic variation in fat content is not surprising since it is frequently seen even in the very small volumes of tissue obtained on liver biopsy. Further, the location of voxels within the liver is unlikely to be identical at different times of MRS despite our best attempts, because the depths of respiratory excursions may vary. Finally, there may be “real” changes over longer periods of time (Table 4). Nevertheless, the relative stability of the data collected over 24 h supports the validity of performing measurements at different times of the day. The MRS measurements taken several months apart show that, while the extent of fatty liver may vary, the levels remain high on repeated assessments. The determinants of longer-term changes remain to be identified.

Subjects with apoB truncations may be susceptible to fatty livers for several reasons. The major cause is the pres-

TABLE 6. VLDL-TG kinetics

Subjects	VLDL-TG mg/dl	VLDL-TG FCR		VLDL-TG PR
		Glycerol pools/h	Palmitate pools/h	Glycerol mg/dl/h
FHBL				
Mean ± SD	29	1.00	0.37	24.4
	23	0.57	0.15	16.2
Controls				
Mean ± SD	47	1.21	0.59	35.7
	46	0.77	0.31	14.9
<i>P</i>	0.217	0.501	0.021	0.123

Palmitate tracer significantly different from glycerol trace  $P < 0.05$ .

ence of the apoB truncation mutations, and the ensuing reduced capacity of the hepatic VLDL-TG exporting system because the gene defects produce several alterations in lipoprotein transport: *a*) reduced secretion rates of apoB-100 (36, 46, 47); *b*) reduced rates of secretion of some of the apoB truncations (48); and *c*) limited capacity of short truncations (<apoB-40) to transport TG (49–52). Despite these defects of the apoB vehicle, the liver VLDL exporting system is able to transport more TG than would be expected from the normal functioning of only one allele of apoB. Smaller numbers of particles and smaller than normal sized particles must be able carry more TG per particle than under normal conditions. However, this adaptation is clearly insufficient to prevent TG accumulation in liver.

Several factors affect the amount of fat accumulated in liver (23). These did not account for the differences between the amounts of liver fat in our FHBL subjects and controls. The two groups did not differ in their intakes of nutrients or alcohol, nor did they differ with respect to indexes of generalized or abdominal obesity, or insulin resistance as measured during an oral glucose tolerance test. To the extent that the oral test underestimates “true” insulin resistance (compared with the “gold standard”, the hyperinsulinemic euglycemic clamp method), we may have missed subtle abnormalities in insulin sensitivity. Thus, the question of insulin resistance in FHBL remains somewhat open. Further, differential rates of flux of free fatty acids to liver could not account for the hepatosteatosis, because rates of flux of fatty acid to liver were similar in the FHBL and control groups. (Rates of palmitate appearance into plasma were similar between groups and the rate of disposal equals the rate of appearance at metabolic steady state). Finally, rates of hepatic VLDL-TG production in FHBL subjects were the same or decreased compared with controls (36, 38), probably reflecting decreased rates of hepatic fatty acid synthesis, as illustrated in the apoB-38.9- and apoB-27.6-bearing mice (51, 52). Thus, the apoB defects per se played major roles in the hepatosteatosis.

The amount of hepatic fat present varies widely between various FHBL subjects. We have also demonstrated variability in the amount of liver fat accumulated in genetically engineered mice with apoB38.9 and apoB27.6 truncations (51–53). In part, this variability may be due to countervailing processes that may limit fat accumulation. These mice manifest fatty livers, along with a concomitant compensatory down-regulation of hepatic fatty acid synthesis and decreased expression of several fatty acid synthetic enzymes and of SREBP-1c, the responsible transcription factor (53). Thus, the amount of TG accumulating in liver is probably modulated by a number of genes. One would predict that “genetic background” on which the apoB truncation is superimposed would affect the degree of hepatic fat accumulation, but this remains to be determined.

The use of palmitate infusions to study the contribution of nonplasma FA sources to VLDL-TG assembly assumes that palmitate is an adequate tracer of other FAs. In pre-

liminary experiments, B. Patterson and S. Klein (unpublished observations) infused five  $^2\text{H}$ -labeled FAs (myristate, palmitate, stearate, oleate, and linoleate) in seven healthy subjects. The Ra of palmitate as a percentage of the sum of all five FAs was constant under basal fasting conditions, and when whole body lipolysis was stimulated or inhibited. Furthermore, the percentage of palmitate and oleate compositions of plasma TG (33% and 41%, respectively) was similar to the percentage composition of plasma NEFA (28% and 39%, nonesterified palmitate and oleate, respectively). Therefore, we believe palmitate to be an adequate tracer for our purposes.

We recently validated the use of stable isotopically labeled glycerol and palmitate tracers to determine the turnover rate of VLDL-TG (37). The two tracers gave the same VLDL-TG FCR when given simultaneously as a bolus, and the metabolic kinetics were analyzed by the compartmental model that could resolve VLDL turnover from tracer recycling. However, the apparent FCR using a constant infusion of labeled palmitate was substantially lower than the “true” FCR obtained using a bolus of glycerol, because the tracer-recycling pathway cannot be resolved with the infused palmitate tracer. The same relationship was observed with the subjects in this study (Table 6). The “true” VLDL-TG FCR measured with the bolus glycerol tracer was not significantly different between FHBL and control subjects, whereas the “apparent” VLDL-TG FCR measured with the infused palmitate was significantly slower in the FHBL subjects who had elevated hepatic lipid levels. The present study confirms our earlier speculation (37) that the VLDL-TG time course using an infusion of palmitate appears slower than the “true” VLDL-TG turnover rate, because palmitate tracer is taken up into a hepatic lipid pool that turns over slowly and contributes a “slow” pathway for tracer incorporation into VLDL-TG palmitate. This intrahepatic pathway for fatty acid tracer recycling causes an attenuation of the VLDL-TG palmitate time course kinetics over how it would appear in the absence of this slowly turning over hepatic lipid pool. It is likely that the infused palmitate tracer may in fact provide more information about the turnover rate of hepatic lipid stores than it does VLDL-TG.

The presence of fatty liver due to a known genetic cause in our FHBL subjects provided the opportunity to examine the relationship between the amounts of fat present in liver and the contributions of nonplasma sources of fatty acids to the assembly of VLDL-TG. Non-plasma sources provided a larger proportion of fatty acids in FHBL subjects than in controls. In addition, the strong correlation observed between the percentage of liver fat by MRS and the contribution of nonplasma sources to VLDL-TG assembly in FHBL subjects strongly suggests that hepatic lipid rather than other splanchnic stores contributes a major portion of nonplasma palmitate in FHBL subjects. Our results for the relative contribution of hepatic fatty acids are compatible with early reports that used constant infusions with radiolabeled palmitate (54, 55), and more recent studies that used [ $^{13}\text{C}_4$ ]palmitate (41); these range from 0–69%. However, since hepatic fat contents were not



reported in previous studies, correlations between liver fat and VLDL-TG assembly were not determined. The quantitative relationships between liver fat and the proportionate contribution from nonplasma fatty acids differed between FHBL and control subjects (Fig. 3) such that there was a relatively weak correlation between the percentage of liver fat and the portion of VLDL-TG palmitate derived from nonplasma sources in control subjects. This suggests that splanchnic lipid stores rather than hepatic fat may provide a greater portion of fatty acids for VLDL-TG production in this group. It remains to be seen whether the quantitative relationship established here for FHBL exists also in other forms of fatty liver, e.g., that associated with obesity and/or insulin resistance. **■**

The authors appreciate the cooperation of our study subjects and the interactions of Jackie Dudley RN and Sherry Banez-Muth RN with them. We are grateful to Tom Kitchens for expert technical assistance, to G. Larry Bretthorst for help with the Bayesian probability theory data analysis, to Xiaobo Lin and Nobuhiro Sakata for the mouse fat determinations, and to Mary Lou Rheinheimer and Patrick Doyle for preparation of the manuscript. This research was supported by National Institutes of Health Grants HL-RO1-59515, HL-R37-42460, RR-00036 (General Clinical Research Center), DK-56341 (Clinical Nutrition Research Unit), RR-00954 (Biomedical Mass Spectrometry Resource) and R24-CA83060 (Small Animal Imaging Resource Program).

## REFERENCES

- Kane, J. P. and R. J. Havel. 1995. Disorders of the biogenesis and secretion of lipoproteins containing the B apolipoproteins. In *The Metabolic and Molecular Bases of Inherited Disease*. C. R. Scriver, A. L. Beaudet, W. S. Sly, and D. Valle, editors. McGraw-Hill Inc., New York. 1853–1885.
- Linton, M. F., R. V. Farese, Jr., and S. G. Young. 1993. Familial hypobetalipoproteinemia. *J. Lipid Res.* **34**: 521–541.
- Schonfeld, G. 1995. The hypobetalipoproteinemias. *Annu. Rev. Nutr.* **15**: 23–34.
- Welty, F. K., J. Ordovas, E. J. Schaefer, P. W. Wilson, and S. G. Young. 1995. Identification and molecular analysis of two apoB gene mutations causing low plasma cholesterol levels. *Circulation.* **92**: 2036–2040.
- Tarugi, P., A. Lonardo, C. Gabelli, F. Sala, G. Ballarini, I. Cortella, L. Previato, S. Bertolini, R. S. Cordera, and S. Calandra. 2001. Phenotypic expression of familial hypobetalipoproteinemia in three kindreds with mutations of apolipoprotein B gene. *J. Lipid Res.* **42**: 1552–1561.
- Yuan, B., R. Neuman, S. H. Duan, J. L. Weber, P. Y. Kwok, N. L. Saccone, J. S. Wu, K. Y. Liu, and G. Schonfeld. 2000. Linkage of a gene for familial hypobetalipoproteinemia to chromosome 3p21.1–22. *Am. J. Hum. Genet.* **66**: 1699–1704.
- Neuman, R. J., B. Yuan, D. R. Gerhard, K. Y. Liu, P. Yue, S. Duan, M. Averna, and G. Schonfeld. 2002. Replication of linkage of familial hypobetalipoproteinemia to chromosome 3p in six kindreds. *J. Lipid Res.* **43**: 407–415.
- Hobbs, H. H., E. Leitersdorf, C. C. Leffert, D. R. Cryer, M. S. Brown, and J. L. Goldstein. 1989. Evidence for a dominant gene that suppresses hypercholesterolemia in a family with defective low density lipoprotein receptors. *J. Clin. Invest.* **84**: 656–664.
- Knoblauch, H., B. Muller-Myhsok, A. Busjahn, L. Ben Avi, S. Bahring, H. Baron, S. C. Heath, R. Uhlmann, H. D. Faulhaber, S. Shpitzen, A. Aydin, A. Reshef, M. Rosenthal, O. Eliav, A. Muhl, A. Lowe, D. Schurr, D. Harats, E. Jeschke, Y. Friedlander, H. Schuster, F. C. Luft, and E. Leitersdorf. 2000. A cholesterol-lowering gene maps to chromosome 13q. *Am. J. Hum. Genet.* **66**: 157–166.
- Wishingrad, M., B. Paaso, and H. Garcia. 1994. Fatty liver due to heterozygous hypobetalipoproteinemia. *Am. J. Gastroenterol.* **89**: 1106–1107.
- Hagve, T. A., L. E. Myrseth, E. Schrupf, J. P. Blomhoff, B. Christophersen, K. Elgjo, E. Gjone, and H. Prydz. 1991. Liver steatosis in hypobetalipoproteinemia. A case report. *J. Hepatol.* **13**: 104–111.
- Castellano, G., C. Garfia, D. Gomez-Coronado, J. Arenas, J. Manzanares, F. Colina, and J. A. Solis-Herruzo. 1997. Diffuse fatty liver in familial heterozygous hypobetalipoproteinemia. *J. Clin. Gastroenterol.* **25**: 379–382.
- Ogata, H., K. Akagi, M. Baba, A. Nagamatsu, N. Suzuki, K. Nomiya, and M. Fujishima. 1997. Fatty liver in a case with heterozygous familial hypobetalipoproteinemia. *Am. J. Gastroenterol.* **92**: 339–342.
- Ahmed, A., and E. B. Keeffe. 1998. Asymptomatic elevation of aminotransferase levels and fatty liver secondary to heterozygous hypobetalipoproteinemia. *Am. J. Gastroenterol.* **93**: 2598–2599.
- Mehta, N. N., and H. G. Desai. 1997. Persistent transaminase elevation due to heterozygous (familial) apolipoprotein B deficiency. *Indian J. Gastroenterol.* **16**: 158–159.
- Tarugi, P., and A. Lonardo. 1997. Heterozygous familial hypobetalipoproteinemia associated with fatty liver. *Am. J. Gastroenterol.* **92**: 1400–1402.
- Tarugi, P., A. Lonardo, G. Ballarini, L. Erspamer, E. Tondelli, S. Bertolini, and S. Calandra. 2000. A study of fatty liver disease and plasma lipoproteins in a kindred with familial hypobetalipoproteinemia due to a novel truncated form of apolipoprotein B (APO B-54.5). *J. Hepatol.* **33**: 361–370.
- Tarugi, P., A. Lonardo, G. Ballarini, A. Grisendi, M. Pulvirenti, A. Bagni, and S. Calandra. 1996. Fatty liver in heterozygous hypobetalipoproteinemia caused by a novel truncated form of apolipoprotein B. *Gastroenterology.* **111**: 1125–1133.
- Szczepaniak, L. S., E. E. Babcock, F. Schick, R. L. Dobbins, A. Garg, D. K. Burns, J. D. McGarry, and D. T. Stein. 1999. Measurement of intracellular triglyceride stores by H spectroscopy: validation in vivo. *Am. J. Physiol.* **276**: E977–E989.
- Ricci, C., R. Longo, E. Gioulis, M. Bosco, P. Pollesello, F. Masutti, L. S. Croce, S. Paoletti, B. de Bernard, C. Tiribelli, and L. Dalla Palma. 1997. Noninvasive in vivo quantitative assessment of fat content in human liver. *J. Hepatol.* **27**: 108–113.
- Longo, R., P. Pollesello, C. Ricci, F. Masutti, B. J. Kvam, L. Bercich, L. S. Croce, P. Grigolato, S. Paoletti, and B. de Bernard. 1995. Proton MR spectroscopy in quantitative in vivo determination of fat content in human liver steatosis. *J. Magn. Reson. Imaging.* **5**: 281–285.
- Falck-Ytter, Y., Z. M. Younossi, G. Marchesini, and A. J. McCullough. 2001. Clinical features and natural history of nonalcoholic steatosis syndromes. *Semin. Liver Dis.* **21**: 17–26.
- Marchesini, G., M. Brizi, A. M. Morselli-Labate, G. Bianchi, E. Bugianesi, A. J. McCullough, G. Forlani, and N. Melchionda. 1999. Association of nonalcoholic fatty liver disease with insulin resistance. *Am. J. Med.* **107**: 450–455.
- Brown, A. M., D. Wiggins, and G. F. Gibbons. 1999. Glucose phosphorylation is essential for the turnover of neutral lipid and the second stage assembly of triacylglycerol-rich ApoB-containing lipoproteins in primary hepatocyte cultures. *Arterioscler. Thromb. Vasc. Biol.* **19**: 321–329.
- Gibbons, G. F., S. M. Bartlett, C. E. Sparks, and J. D. Sparks. 1992. Extracellular fatty acids are not utilized directly for the synthesis of very-low-density lipoprotein in primary cultures of rat hepatocytes. *Biochem. J.* **287**: 749–753.
- Schonfeld, G., and B. Pflieger. 1971. Utilization of exogenous free fatty acids for the production of very low density lipoprotein triglyceride by livers of carbohydrate-fed rats. *J. Lipid Res.* **12**: 614–621.
- Hamilton, R. L., J. S. Wong, C. M. Cham, L. B. Nielsen, and S. G. Young. 1998. Chylomicron-sized lipid particles are formed in the setting of apolipoprotein B deficiency. *J. Lipid Res.* **39**: 1543–1557.
- Raabe, M., M. M. Veniant, M. A. Sullivan, C. H. Zlot, J. Bjorkegren, L. B. Nielsen, J. S. Wong, R. L. Hamilton, and S. G. Young. 1999. Analysis of the role of microsomal triglyceride transfer protein in the liver of tissue-specific knockout mice. *J. Clin. Invest.* **103**: 1287–1298.
- Schonfeld, G., J. Ackerman, and D. Yablonskiy. 2001. Fatty liver in familial hypobetalipoproteinemia (FHBL). *Arterioscler. Thromb. Vasc. Biol.* **21**: 656.
- Yablonskiy, D. A., J. J. Ackerman, and G. Schonfeld. 2001. Liver-fat



- content quantification by MR spectroscopy in patients with apoB truncation-containing lipoproteins (Abstract). *Radiology*. **221**: 496.
31. Bottomley, P. A. 1987. Spatial localization in NMR spectroscopy in vivo. *Ann. N. Y. Acad. Sci.* **508**: 333–348.
32. Raddi, A., and U. Klose. 1998. A generalized estimate of the SLR B polynomial ripples for RF pulse generation. *J. Magn. Reson.* **132**: 260–265.
33. Bretthorst, G. L. 1988. Bayesian Spectrum Analysis and Parameter Estimation. Lecture Notes in Statistics. Springer-Verlag, Berlin.
34. Thomsen, C., U. Becker, K. Winkler, P. Christoffersen, M. Jensen, and O. Henriksen. 1994. Quantification of liver fat using magnetic resonance spectroscopy. *Magn. Reson. Imaging*. **12**: 487–495.
35. Bligh, E., and W. Dyer. 1959. A rapid method of total lipid extraction and purification. *Can. J. Biochem. Physiol.* **37**: 911–917.
36. Elias, N., B. W. Patterson, and G. Schonfeld. 1999. Decreased production rates of VLDL triglycerides and ApoB-100 in subjects heterozygous for familial hypobetalipoproteinemia. *Arterioscler. Thromb. Vasc. Biol.* **19**: 2714–2721.
37. Patterson, B. W., B. Mittendorfer, N. Elias, R. Satyanarayana, and S. Klein. 2002. Use of stable isotopically labeled tracers to measure very low density lipoprotein-triglyceride turnover. *J. Lipid Res.* **43**: 223–233.
38. Elias, N., B. W. Patterson, and G. Schonfeld. 2000. In vivo metabolism of ApoB, ApoA-I, and VLDL triglycerides in a form of hypobetalipoproteinemia not linked to the ApoB gene. *Arterioscler. Thromb. Vasc. Biol.* **20**: 1309–1315.
39. Hudgins, L. C., M. Hellerstein, C. Seidman, R. Neese, J. Diakun, and J. Hirsch. 1996. Human fatty acid synthesis is stimulated by a eucaloric low fat, high carbohydrate diet. *J. Clin. Invest.* **97**: 2081–2091.
40. Aarsland, A., and R. R. Wolfe. 1998. Hepatic secretion of VLDL fatty acids during stimulated lipogenesis in men. *J. Lipid Res.* **39**: 1280–1286.
41. Parks, E. J., R. M. Krauss, M. P. Christiansen, R. A. Neese, and M. K. Hellerstein. 1999. Effects of a low-fat, high-carbohydrate diet on VLDL-triglyceride assembly, production, and clearance. *J. Clin. Invest.* **104**: 1087–1096.
42. Lemieux, S., B. W. Patterson, A. Carpentier, G. F. Lewis, and G. Steiner. 1999. A stable isotope method using a [(2)H(5)]glycerol bolus to measure very low density lipoprotein triglyceride kinetics in humans. *J. Lipid Res.* **40**: 2111–2117.
43. Steele, R. 1959. Influences of glucose loading and of injected insulin on hepatic glucose output. *Ann. N. Y. Acad. Sci.* **82**: 420–430.
44. Rosenblatt, J., and R. R. Wolfe. 1988. Calculation of substrate flux using stable isotopes. *Am. J. Physiol.* **254**: E526–E531.
45. Matthews, D. R., J. P. Hosker, A. S. Rudenski, B. A. Naylor, D. F. Treacher, and R. C. Turner. 1985. Homeostasis model assessment: insulin resistance and beta-cell function from fasting plasma glucose and insulin concentrations in man. *Diabetologia*. **28**: 412–419.
46. Aguilar-Salinas, C. A., P. H. Barrett, K. G. Parhofer, S. G. Young, D. Tessereau, J. Bateman, C. Quinn, and G. Schonfeld. 1995. Apoprotein B-100 production is decreased in subjects heterozygous for truncations of apoprotein B. *Arterioscler. Thromb. Vasc. Biol.* **15**: 71–80.
47. Welty, F. K., A. H. Lichtenstein, P. H. Barrett, G. G. Dolnikowski, J. M. Ordovas, and E. J. Schaefer. 1997. Decreased production and increased catabolism of apolipoprotein B-100 in apolipoprotein B-67/B-100 heterozygotes. *Arterioscler. Thromb. Vasc. Biol.* **17**: 881–888.
48. Parhofer, K. G., P. H. Barrett, C. A. Aguilar-Salinas, and G. Schonfeld. 1996. Positive linear correlation between the length of truncated apolipoprotein B and its secretion rate: in vivo studies in human apoB-89, apoB-75, apoB-54.8, and apoB-31 heterozygotes. *J. Lipid Res.* **37**: 844–852.
49. Groenewegen, W. A., M. R. Averna, J. Pulai, E. S. Krul, and G. Schonfeld. 1994. Apolipoprotein B-38.9 does not associate with apo[a] and forms two distinct HDL density particle populations that are larger than HDL. *J. Lipid Res.* **35**: 1012–1025.
50. Talmud, P. J., E. S. Krul, M. Pessah, G. Gay, G. Schonfeld, S. E. Humphries, and R. Infante. 1994. Donor splice mutation generates a lipid-associated apolipoprotein B-27.6 in a patient with homozygous hypobetalipoproteinemia. *J. Lipid Res.* **35**: 468–477.
51. Chen, Z., R. L. Fitzgerald, M. R. Averna, and G. Schonfeld. 2000. A targeted apolipoprotein B-38.9-producing mutation causes fatty livers in mice due to the reduced ability of apolipoprotein B-38.9 to transport triglycerides. *J. Biol. Chem.* **275**: 32807–32815.
52. Chen, Z., R. L. Fitzgerald, and G. Schonfeld. 2002. Hypobetalipoproteinemic mice with a targeted apolipoprotein (Apo) B-27.6-specifying mutation: in vivo evidence for an important role of amino acids 1254–1744 of ApoB in lipid transport and metabolism of the apoB-containing lipoprotein. *J. Biol. Chem.* **277**: 14135–14145.
53. Lin, X., G. Schonfeld, and Z. Chen. 2001. Molecular adaptation of the fatty acid synthetic pathway to the presence of fatty livers in gene-targeted mice producing apolipoprotein B-39.8 (Abstract). *Arterioscler. Thromb. Vasc. Biol.* **21**: 661.
54. Barter, P. J., and P. J. Nestel. 1973. Precursors of plasma triglyceride fatty acids in obesity. *Metabolism*. **22**: 779–783.
55. Barter, P. J., P. J. Nestel, and K. F. Carroll. 1972. Precursors of plasma triglyceride fatty acid in humans. Effects of glucose consumption, clofibrate administration, and alcoholic fatty liver. *Metabolism*. **21**: 117–124.
56. Pulai, J. I., H. Zakeri, P. Y. Kwok, J. H. Kim, J. Wu, and G. Schonfeld. 1998. Donor splice mutation (665 + 1 G<sub>T</sub>) in familial hypobetalipoproteinemia with no detectable apoB truncation. *Am. J. Med. Genet.* **80**: 218–220.
57. Wu, J., J. Kim, Q. Li, P. Y. Kwok, T.G. Cole, B. Cefalu, M. Averna, and G. Schonfeld. 1999. Known mutations of apoB account for only a small minority of hypobetalipoproteinemia. *J. Lipid Res.* **40**: 955–959.
58. Yue, P., B. Yuan, D. S. Gerhard, R. J. Neuman, W. L. Isley, W. S. Harris, and G. Schonfeld. 2002. Novel mutations of APOB cause ApoB truncations undetectable in plasma and familial hypobetalipoproteinemia. *Hum. Mutat.* **20**: 110–116.
59. Young, S. G., S. T. Hubl, R. S. Smith, S. M. Snyder, and J. F. Terdiman. 1990. Familial hypobetalipoproteinemia caused by a mutation in the apolipoprotein B gene that results in a truncated species of apolipoprotein B (B-31). A unique mutation that helps to define the portion of the apolipoprotein B molecule required for the formation of buoyant, triglyceride-rich lipoproteins. *J. Clin. Invest.* **85**: 933–942.
60. Groenewegen, W. A., E. S. Krul, and G. Schonfeld. 1993. Apolipoprotein B-52 mutation associated with hypobetalipoproteinemia is compatible with a misaligned pairing deletion mechanism. *J. Lipid Res.* **34**: 971–981.
61. Wagner, R. D., E. S. Krul, J. Tang, K. G. Parhofer, K. Garlock, P. Talmud, and G. Schonfeld. 1991. ApoB-54.8, a truncated apolipoprotein found primarily in VLDL, is associated with a nonsense mutation in the apoB gene and hypobetalipoproteinemia. *J. Lipid Res.* **32**: 1001–1011.
62. Krul, E. S., K. G. Parhofer, P. H. Barrett, R. D. Wagner, and G. Schonfeld. 1992. ApoB-75, a truncation of apolipoprotein B associated with familial hypobetalipoproteinemia: genetic and kinetic studies. *J. Lipid Res.* **33**: 1037–1050.
63. Talmud, P., L. King-Underwood, E. Krul, G. Schonfeld, and S. Humphries. 1989. The molecular basis of truncated forms of apolipoprotein B in a kindred with compound heterozygous hypobetalipoproteinemia. *J. Lipid Res.* **30**: 1773–1779.